©2004 FASEB

***The FASEB Journal*** express article 10.1096/fj.03-1349fje. Published online September 2, 2004.

# The N-terminal copper-binding domain of the amyloid precursor protein protects against $Cu^{2+}$ neurotoxicity in vivo

Waldo F. Cerpa,* María I. Barría,* Marcelo A. Chacón,* Miriam Suazo,[†] Mauricio González,[†] Carlos Opazo,*[,‡] Ashley I. Bush,[‡,§] and Nibaldo C. Inestrosa*

*Centro FONDAP de Regulación Celular y Patología "Joaquín V. Luco," MIFAB, Facultad de Ciencias Biológicas, Pontificia Universidad Católica de Chile; [†]Instituto de Nutrición y Tecnología de Alimentos, Universidad de Chile, Santiago, Chile; [‡]Mental Health Research Institute of Victoria, Parkville, 3010 Parkville, Victoria, Australia; and [§]Genetics and Aging Research Unit, Harvard Medical School, Massachusetts General Hospital, Charlestown, Massachusetts 02129

Corresponding author: Dr. Nibaldo C. Inestrosa, FONDAP-Biomedical Center, P. Universidad Católica de Chile, Alameda 340, Santiago, Chile. E-mail: ninestr@genes.bio.puc.cl

Waldo F. Cerpa and María I. Barría contributed equally to this work.

## ABSTRACT

The amyloid precursor protein (APP) contains a Cu binding domain (CuBD) localized between amino acids 135 and 156 ($APP_{135-156}$), which can reduce $Cu^{2+}$ to $Cu^{1+}$ in vitro. The physiological function of this APP domain has not yet being established; nevertheless several studies support the notion that the CuBD of APP is involved in Cu homeostasis. We used APP synthetic peptides to evaluate their protective properties against $Cu^{2+}$ neurotoxicity in a bilateral intra-hippocampal injection model. We found that human $APP_{135-156}$ protects against $Cu^{2+}$-induced neurotoxic effects, such as, impairment of spatial memory, neuronal cell loss, and astrogliosis. $APP_{135-156}$ lacking two histidine residues showed protection against $Cu^{2+}$; however, $APP_{135-156}$ mutated in cysteine 144, a key residue in the reduction of $Cu^{2+}$ to $Cu^{1+}$, did not protect against $Cu^{2+}$ neurotoxicity. In accordance with recent reports, the CuBD of the *Caenorhabditis elegans*, APL-1, protected against $Cu^{2+}$ neurotoxicity in vivo. We also found that $Cu^{2+}$ neurotoxicity is associated with an increase in nitrotyrosine immunofluorescence as well as with a decrease in $Cu^{2+}$ uptake. The CuBD of APP therefore may play a role in the detoxification of brain Cu.

Key words: water maze • intracerebral injection

The amyloid precursor protein (APP) is a cell surface transmembrane glycoprotein containing the amyloid-β peptide, which is involved in the pathogenesis of Alzheimer's disease (AD) (1). APP possesses two Cu binding domains (CuBD): one located in the C-terminal region within the amyloid-β peptide (2) and the other located in its N-terminal region between residues 135 and 156; this region can bind $Cu^{2+}$ and reduce it to $Cu^{1+}$ in vitro (3), Cys 144 being a key residue in this process (4). APP is a member of a multigene family that contains the amyloid precursor-like proteins (APPL1 and APPL2; refs 5, 6). Moreover, nonmammalian APP orthologs have been identified in a diverse range of species, including *Caenorhabditis*

*elegans* (7). The CuBD sequence is similar among the members of APP family, suggesting an overall conservation on its function or activity.

The normal function of APP is unknown; however, several trophic functions have been suggested for soluble APP (8–13). In relation to Cu metabolism, it has been suggested that Cu transport from the extracellular to the intracellular compartment may be mediated by APP (3, 4, 14). Various studies have suggested that APP has a role in Cu homeostasis (4, 15–18). APP and APLP2 knockout mice show specific elevations in $Cu^{2+}$ levels of cerebral cortex and liver (15), while APP transgenic mice (Tg2576) have decreased $Cu^{2+}$ levels in brain (17).

In this work, we have studied the effect of the N-terminal CuBD of APP on $Cu^{2+}$ neurotoxicity in vivo. We injected $CuCl_2$ with CuBD synthetic peptides in the rat hippocampus, and the behavioral changes were evaluated by the Morris water maze task. The hippocampal damage was evaluated by examining neuronal cell loss and astrogliosis. We found that both human wild-type $APP_{135-156}$ and a mutant $APP_{135-156}$ lacking of the histidine residues involved in the Cu binding (His147 and His149) were neuroprotective against $CuCl_2$ toxicity. However, the CuBD APP peptide lacking Cys144 (involved in the reduction of $Cu^{2+}$ to $Cu^{1+}$) was not protective against $CuCl_2$ neurotoxicity. In accordance with previous studies (16), CuBD of *C. elegans* APL-1, protected against $CuCl_2$ toxicity in vivo. Moreover, we found that the differences in protection against $Cu^{2+}$ neurotoxicity may be due to an altered response to oxidative stress. Interestingly, differences in $Cu^{2+}$ uptake were also observed, with a higher $Cu^{2+}$ uptake when $CuCl_2$ was injected in the presence of the neuroprotective peptides. Our results are consistent with the idea that APP is involved in the modulation of Cu homeostasis in vivo.

## MATERIALS AND METHODS

### Synthetic peptides

Peptide corresponding to the human wild-type $APP_{135-156}$ sequence (CuBD) was obtained from Chiron Corp. (Emeryville, CA). Variant APP peptides containing a Cys→Ser substitution ($APP_{Cys144\rightarrow Ser}$), and a double His→Ala substitution at positions 147 and 149 ($APP_{His147\rightarrow Ala/His149\rightarrow Ala}$), were obtained from BioSynthesis Inc. (Lewisville, TX). The corresponding CuBD of *C. elegans* APL-1 ($APP_{135-156}$ *C. elegans*) was obtained from Genemed Biotechnologies, Inc. (San Francisco, CA). Histidine was from Merck (Darmstadt, Germany). Stock solutions (1 mg/ml) were prepared by dissolving the peptides directly in artificial cerebrospinal fluid (aCSF) containing 130 mM NaCl, 2.6 mM KCl, 4.3 mM $MgCl_2$, and 1.8 mM $CaCl_2$, pH 7.4.

### Incubation of peptides before the injection

Synthetic peptides were mixed with $CuCl_2$ at 5.0 μM final concentration and were incubated overnight at 4°C or incubated overnight at 37°C and injected bilaterally into the dorsal hippocampus (incubation treatment: I); also peptides were mixed and immediately injected (without incubation treatment: WI). In addition, we carried out metallation of the peptides (dialysis treatment) as described by White and co-workers (16). Briefly, synthetic peptides (150 μl sample, 10 μM) were mixed with $CuCl_2$ (150 μl sample, 10 μM); the mixtures were incubated overnight at 37°C and then dialyzed using mini-dialysis cups (500 Da cutoff) (Spectrum

Laboratories, Inc., Rancho Dominguez, CA) for 24 h against two changes of aCSF (300 ml per change) at 20°C. The final peptide concentration was determined by a micro BCA protein assay (Pierce Biotechnology, Inc., Rockford, IL).

## Surgical and injection protocol

Male Sprague-Dawley rats (300 g, 3 months old) were anesthetized with Equitesin (3.5 ml/Kg i.p.) and injected bilaterally into the dorsal hippocampus (-3.5 mm AP, ±2.0 mm ML and -2.7 mm DV, according to Bregma) following the Paxinos and Watson (19) indications, stereotaxically with a 10 μl Hamilton syringe with 27-gauge stainless steel. Animals were injected bilaterally with 3 μl (at rate of 0.5 μl/min) of 5.0 μM $CuCl_2$, in the presence or absence of 5.0 μM CuBD APP peptides in different conditions as described above; aCSF was used as vehicle. Four days after intracerebral injection, rats were trained in the Morris water maze for 2 wk and the performance of the different groups was recorded for analysis. After training, the animals were fixed by intracardiac perfusion to carry out the histochemical procedures.

## Behavioral test

All animals were trained in a circular water maze (1.6 m diameter and 75 cm deep, painted black) (20) using a two trial per day regimen. The platform (9 cm diameter) always resided in the center of northwest quadrant (hidden platform quadrant). Water (50 cm deep) was maintained at 19-21°C. Data were gathered with a video tracking system for water maze (HVS Imagem, Hampton, UK). Briefly, rats were trained with two trials a day, for 5 consecutive days, followed by 2 days off, and then trained for 5 additional days. Each trial began when rats were allowed to swim. A trial continued until the animal was put onto the platform for 5 s and returned to its cage. Upon completion of all two trials, rats were removed from the maze, dried, and returned to their cage.

## Perfusion and fixation

Animals were anesthetized with Equitesin (3.5 ml/kg ip) before perfusion. Rats were perfused through the heart with saline (0.9% NaCl) followed by fixation with 4% paraformaldehyde in 0.1 M phosphate buffer saline (PBS). Brains were removed from their skulls and postfixed in the same fixative for 3 h at room temperature, followed by 20% sucrose in PBS at 4°C overnight. After fixation, brains were coded to ensure unbiased processing and analysis. The brains were then cut into 30 μm coronal sections with a cryostat (Leitz 1900) at -20°C, from Bregma -1.8 mm to Bregma -4.8 mm (19). Sections from the same brain were divided in groups for analysis of the Nissl staining (0.3% cresyl violet) and the glial fibrillary acidic protein (GFAP) immunohistochemical staining.

## Immunohistochemical staining

Free-floating immunohistochemical procedure was performed as described previously (21). Washing and dilution of immunoreagents was performed with 0.01 M PBS plus 0.2% Triton X-100 (PBS+T) throughout the experiments, and two PBS+T washes were performed between every antibody incubation. Sections were pretreated with 0.5% $H_2O_2$ for 30 min to reduce endogenous peroxidase activity followed by incubation with 3% bovine serum albumin (BSA) at

room temperature for 1 h to avoid nonspecific binding. GFAP detection was performed using a rabbit anti-GFAP (1:500) polyclonal antibody incubated overnight at 4°C. A horseradish peroxidase (HRP)-conjugated goat anti-rabbit IgG secondary antibody (1:600) was used in GFAP detection incubated for 1 h at room temperature. The staining was developed by incubation with 0.06% diaminobenzidine during 15 min followed by addition of $H_2O_2$ (0.01% final concentration) and incubation for 4 min. After immunostaining, all sections were mounted on gelatin-coated slides, air-dried, dehydrated by serial rinses in graded ethanol solutions, cleared with xilene, and cover-slipped with Canada balsam (Merck, Darmstadt, Germany).

**Immunofluorescence detection of nitrotyrosine**

Fixed brain sections mounted in slides were washed with PBS and PBS+T, and followed by glycine (0.15 M) and $NaBH_4$ (10 mg/ml) incubations to decrease the background of the reaction. Sections were washed again with PBS and PBS+T and then followed by treatment with 3% BSA at room temperature for 1.5 h to avoid nonspecific binding. Nitrotyrosine detection was performed using an anti-nitrotyrosine (1:100) rabbit immunoaffinity purified IgG antibody (Upstate Biotechnology, Lake Placid, NY), incubated overnight at 4°C. After being washed with PBS+T containing 0.5% BSA, sections were incubated for 2 h at room temperature with an anti-rabbit IgG-FITC second antibody (1:500). The sections were washed with PBS+T in 0.5% BSA, PBS and finally water. The slides were cover-slipped with fluorescent mounting medium (DAKO, Carpinteria, CA).

**Nissl staining**

Mounted sections were defatted in xylene and hydrated in ethyl alcohol and water series. Nissl staining (cresyl violet) was performed as described previously (21).

**Image analysis**

The number of the cells in the injection site was quantified with the program Image Pro-Express (Carlsbad, CA); digital quantification of nitrotyrosine staining area was measured with Image Tool software (San Antonio, TX). The number of reactive astrocytes, intensity of staining in the soma, and size of the astrocyte soma were quantified with SigmaScan Pro software (Chicago, IL). All the analysis was carried out with at least three x40 pictures of the injection site per treatment.

**Measurement of $^{64}$Cu uptake**

Radioactive [$^{64}\gamma$]Cu as $CuSO_4$ salt was purchased from the Chilean Commission of Nuclear Energy, Santiago, Chile. $Cu^{2+}$ uptake experiments were performed on rats injected in the hippocampus with 50 μM [$^{64}\gamma$]Cu (specific activity 4.1 mCi/mg) plus the different synthetic APP peptides; after 14 h, animals were anesthetized with ethyl ether and the brains were removed from their skulls and the hippocampus was dissected and kept on ice. The uptake experiment was stopped with cold PBS supplemented with 1 mM EDTA and with an excess of Cu-His (1:10). The hippocampus was disrupted by homogenization with 600 μl of 0.5 N NaOH, 0.1% Triton X-100. The [$^{64}\gamma$]Cu cellular content was determined by measuring the radioactivity in 550 μl aliquots of the lysate with a γ-counter (Packard 1600TR), and the concentration was interpolated

from a standard curve of 1 -100 pmol of [$^{64}\gamma$]Cu. In addition a sample was separated for protein determination by the Bradford method (22).

### Statistical analysis

All results were expressed as means ± SE. Two-way ANOVA was also conducted for analyzing data of the water maze. $P < 0.05$ was regarded as statistically significant.

## RESULTS

### $APP_{135-156}$ protects spatial memory against $Cu^{2+}$ toxicity

The human CuBD was used to evaluate its ability to prevent the behavioral impairment caused by the intrahippocampal injection of $CuCl_2$. Rats injected with $CuCl_2$ (5 μM) alone showed spatial memory impairments (Fig. 1*A*); however, animals co-injected with 5 μM $CuCl_2$ and 5 μM of human $APP_{135-156}$ previously incubated for 24h at 4°C behaved like control animals (aCSF injected rats) along the two weeks of training. The protective effect of human $APP_{135-156}$ against $Cu^{2+}$ neurotoxicity was observed also with two other protocols of incubation: *1*) without preincubation, APP peptide was mixed with $CuCl_2$ and immediately injected; and *2*) with preincubation and dialysis (see Materials and Methods) (Fig. 1*B*). Therefore, $APP_{135-156}$ in the same molar ratio with $CuCl_2$ protects against $Cu^{2+}$ neurotoxicity. Representative swimming paths at day 8 of training for all each experimental condition are shown in Fig. 1*C*. These results indicate that human $APP_{135-156}$ protects spatial memory against $Cu^{2+}$ neurotoxicity.

### $APP_{135-156}$ diminishes neuronal cell loss and astrogliosis induced by $CuCl_2$ injection

Rats injected with $APP_{135-156}$ and $CuCl_2$ in all the pre-incubation conditions studied, showed partial neuroprotection of hippocampal morphology, evidenced by a thickening of the upper leaf of the dentate gyrus (DG) (Fig. 2*C*, *D*, *E*) in comparison with $CuCl_2$ injection, which induced an increased thinning of the upper leaf of the DG (Fig. 2*B*). In agreement with this, the quantification of the neuronal cell density in the upper leaf of DG shown a major number of cells in the hippocampus injected with $APP_{135-156}$ and $CuCl_2$ than $CuCl_2$ alone (Fig. 2*J*). The analysis of the astrogliosis showed that the co-injection of human $APP_{135-156}$ with $CuCl_2$ induced only a small astrocytic reaction around the injection site (Fig. 3*C*, *D*, *E*), in comparison with the $CuCl_2$ injection alone (Fig. 2*B*) in all the pre-incubation conditions. The presence of hypertrophic astrocytes was analyzed with SigmaScan Pro software using x40 magnification pictures of different rats. The density of reactive astrocytes (Fig. 3*J*), the intensity of GFAP staining in the soma (Fig. 3*K*), and the size of the reactive astrocyte soma (Fig. 3*L*) were measured. As observed in the Fig. 3*J*, the injection of $CuCl_2$ induced an increase in the density of reactive astrocytes in the injection site, mainly in the upper leaf of the dentate gyrus. Also, the analysis of the intensity of GFAP staining in the astrocyte soma revealed an increased intensity in animals injected with $CuCl_2$ (Fig. 3*K*). Finally, the measurement of the size of the astrocyte soma showed that injection of $CuCl_2$ induced a significative enlargement of the soma (Fig. 3*L*). In contrast, the co-injection of $APP_{135-156}$ with $CuCl_2$ showed a significative decrease on the density of reactive astrocytes, intensity of GFAP staining and size of the reactive astrocyte soma (Fig. 3*J–L*). These results indicate that the CuBD of human APP can prevent, at least partially, the neuronal cell

loss, the astrogliosis and the appearance of hypertrophic astrocytes in the rat hippocampus induced by $CuCl_2$.

### Cysteine is a key residue involved in the neuroprotective effects of $APP_{135-156}$ against $Cu^{2+}$ neurotoxicity

It has been previously shown that the N-terminal region of APP is able to bind and reduce $Cu^{2+}$ to $Cu^{1+}$ (3, 4, 23). To elucidate which of these APP biochemical properties were responsible for the neuroprotective effects of $APP_{135-156}$, we used synthetic peptides without the Cu binding residues ($APP_{His147\rightarrow Ala/His149\rightarrow Ala}$) or without the Cu-reducing residue ($APP_{Cys144\rightarrow Ser}$). Rats injected with $CuCl_2$ plus $APP_{His147\rightarrow Ala/His149\rightarrow Ala}$ (incubated overnight at 4°C) showed protection of spatial memory (Fig. 4*A*; see Fig. 4*E* for representative swimming paths for each treatment at day 8 of training), as also occurs with rats co-injected with $CuCl_2$ and the wild-type $APP_{135-156}$ (see Fig. 1*A*). The same neuroprotective effect was observed with $APP_{His147\rightarrow Ala/His149\rightarrow Ala}$ when it was pre-incubated with $CuCl_2$, dialyzed and then injected (Fig. 4*B*). These results strongly suggest that the $CuCl_2$ binding ability of the N-terminal domain of human APP is not strictly involved in the neuroprotection observed in this model. Nissl staining of hippocampal sections of rats co-injected with $CuCl_2$ and $APP_{His147\rightarrow Ala/His149\rightarrow Ala}$ in conditions of pre-incubation or dialysis did not show important neuronal cell loss in the upper leaf of the DG (Fig. 2*G*), indicating that this peptide was able to prevent the neuronal cell loss induced by $CuCl_2$ (for comparison see Fig. 2*B*), which was confirmed in a digital quantification of the neuronal cell density (Fig. 2*J*). Co-injection of $CuCl_2$ and $APP_{His147\rightarrow Ala/His149\rightarrow Ala}$ induced a lower astrocytic response around the injection site (Fig. 3*F* and *G*), indicating that this peptide is able to decrease this reaction and to diminish the hypertrophic astrocytes induced by $CuCl_2$ injection in all the evaluated conditions. It was also observed in a digital quantification of reactive astrocytes density (Fig. 3*J*), intensity of GFAP staining in the soma (Fig. 3*K*), and the size of the reative astrocyte soma (Fig. 3*L*). On the other hand, rats co-injected with $CuCl_2$ and $APP_{Cys144\rightarrow Ser}$ present higher escape latency values in the memory task close to the values observed by the rats injected with $CuCl_2$ alone. The absence of protection by $APP_{Cys144\rightarrow Ser}$ against $Cu^{2+}$ neurotoxicity was independent of the pre-incubation protocol used (Fig. 4*C* and *D*), which was corroborated by quantification of neuronal cell density by Nissl staining (Fig. 2*H*, *I*, and *J*). Moreover, immunodetection of GFAP showed a strong astrogliosis and hypertrophic astrocytes around the injection site, in all the conditions evaluated (Fig. 3*H* and *I*). It was also observed in a quantification of the reactive astrocytes (Fig. 3*J–L*). These results suggest that Cu-reduction by the CuBD of APP is involved in the neuroprotective effects observed.

### Specific neuroprotective effects of $APP_{135-156}$ against $Cu^{2+}$ neurotoxicity

To analyze specific neuroprotective effect of $APP_{135-156}$ against Copper neurotoxicity, we injected different metals with $APP_{135-156}$. After $ZnCl_2$ and $CdCl_2$ injection only $CdCl_2$ induced an important neuronal cell loss (Fig. 5*B*) and astrogliosis (Fig. 5*D*). $ZnCl_2$ alone does not induced a significant neuronal cell loss. When animals were injected with the above metals plus $APP_{135-156}$, we do not observed differences between animals injected with the metal alone and animals injected with the metal plus $APP_{135-156}$ (compare Fig. 5*A–D* with Fig. 5*E–H*). The graph of quantification of neuronal cell loss did not show difference between animals injected with $APP_{135-156}$ in the absence (Fig. 5*I*) or presence of $ZnCl_2$ or $CdCl_2$. Figure 5*J–L* shows similar

effect, i.e., $APP_{135-156}$ did not change the effect of $ZnCl_2$ or $CdCl_2$ on the appearance of GFAP positive reactive astrocytes. On the other hand, the specificity of the $APP_{135-156}$ effect on copper neurotoxicity as a result of the reduction properties of the APP fragment, were determined by injection of a Histidine, a copper chelator. Only a partial protective effect of Histidine was observed, and this effect was clearly smaller than the one observed by the $APP_{135-156}$ injection (Fig. 5*O–R*), at the level of the neuronal cell loss (Fig. 5*M*) and astrogliosis (Fig. 5*N*).

The dose response data was carried out, and the protection effect with $APP_{135-156}$ is in fact depending of the concentration of APP incubated with copper (Supplement data)

## The CuBD of *C. elegans* APL-1 protects spatial memory against $Cu^{2+}$ neurotoxicity

To determine whether an APP homologue with variations within the central histidine binding site, but keeping the adjacent cysteine intact can protect against $Cu^{2+}$ toxicity, we used the *C. elegans* CuBD ($APP_{135-156\ C.\ elegans}$). This peptide was metallated by incubation with $CuCl_2$ and then dialyzed against aCSF to remove unbound $Cu^{2+}/Cu^{+}$ or mixed with $CuCl_2$ and immediately injected. Rats co-injected with $CuCl_2$ and $APP_{135-156\ C.\ elegans}$ showed an escape latency score similar to control rats, which was independent to the incubation protocol used (Fig. 6*A*; Fig. 6*K* shows a representative swimming paths for each treatment at day 8 of training). To analyze another sensitive spatial memory parameter, we calculated the "spatial acuity." This parameter was obtained after multiplication the percentage of animals present in the quadrant corresponding to the hidden platform (sec) by the percentage of animals present into the platform annulus (sec) (24, 25). Then, we calculated the mean of 10 trials of the water maze acquisition and plotted the escape latency vs. spatial acuity. Figure 6*B* shows that animals co-injected with $CuCl_2$ and $APP_{135-156\ C.\ elegans}$ in the two conditions of incubation are closer to the negative control animals (aCSF injection) than to the positive control ($CuCl_2$). Nissl staining of brain sections of rats co-injected with $CuCl_2$ and $APP_{135-156\ C\ .elegans}$ showed partial neuroprotection against $Cu^{2+}$ neurotoxicity (Fig. 6*C* and *D*) in comparison with $CuCl_2$ alone (see Fig. 2*B*); it was also observed in the quantification of neuronal cell density in the different conditions (Fig. 6*E*). The immunodetection of GFAP showed a lower astrogliosis and a decrease of hypertrophic astrocytes induced by $CuCl_2$ around the injection site in the two treatments carried out (Fig. 6*F* and *G*), in comparison with the animals injected with $CuCl_2$ alone (see Fig. 3*B*). Moreover, a digital analysis of the reactive astrocytes was in agreement with the GFAP immunohistochemistry (Fig. 6*H–J*). These results suggest that the CuBD of the *C. elegans* APP and the CuBD of human APP shares neuroprotective activities against $Cu^{2+}$ neurotoxicity, despite their primary structure differences, suggesting a conserved function for this APP fragment through out evolution.

## CuBD of APP prevents protein tyrosine nitration induced by $CuCl_2$

To determine whether the neuroprotective effect of APP against $CuCl_2$ neurotoxicity is mediated by an antioxidant pathway, we performed a nitrotyrosine immunodetection as an oxidative marker in the injection site of the animals, because it is well known that protein tyrosine nitration is an important marker of oxidative stress (26). The anti-nitrotyrosine staining was carried out 1 wk after the intrahippocampal injection. Results indicate that the injection of aCSF did not show any positive signal (Fig. 7*A*). On the other hand, $CuCl_2$ injection induced a clear signal for protein tyrosine nitration (Fig. 7*B*). In agreement with our previous results, the co-injection of

$CuCl_2$ and $APP_{135\text{-}156}$ present low levels of detection of nitrotyrosine signal (Fig. 7*C*). When the $APP_{Cys144\rightarrow Ser}$ was co-injected with $CuCl_2$ the protein nitration signal was increased (Fig. 7*D*). Both, $CuCl_2$ plus $APP_{His147\rightarrow Ala/His149\rightarrow Ala}$ and $CuCl_2$ plus the APP fragment of *C. elegans* injections, present low levels of nitrotyrosine protein detection (Fig. 7*E* and *F*, respectively). These data show that the formation of nitrotyrosine proteins is a downstream effect of the $Cu^{2+}$ neurotoxicity, which is abolished by the presence of the CuBD of APP, through a mechanism that involves $Cu^{2+}/Cu^{1+}$ reduction.

### CuBD of APP increases $Cu^{2+}$ uptake

To determine if differences in protection against $Cu^{2+}$ neurotoxicity by the CuBD peptides may be related to differences in $Cu^{2+}$ uptake, we co-injected 50 μM $^{64}CuSO_4$ and 50 μM of the different CuBD peptides of APP ($APP_{135\text{-}156}$, $APP_{His147\rightarrow Ala/His149\rightarrow Ala}$, $APP_{Cys144\rightarrow Ser}$ and $APP_{135\text{-}156\ C.elegans}$) and 14 h after the injection, $Cu^{2+}$ uptake was determined. Results show a 10-fold increase in the $Cu^{2+}$ uptake in the presence of human $APP_{135\text{-}156}$ (Fig. 8*A*). In contrast, $APP_{Cys144\rightarrow Ser}$ exhibited only a half effect of its wild-type counterpart in the $Cu^{2+}$ uptake (Fig. 8*B*). Both $APP_{His147\rightarrow Ala/His149\rightarrow Ala}$ and $APP_{135\text{-}156\ C.elegans}$ induced an enhancement in $Cu^{2+}$ uptake (Fig. 8*B*). These data are consistent with the idea that APP protects against $Cu^{2+}$ neurotoxicity by inhibiting the formation of reactive oxygen species by a direct modulation of the $Cu^{2+}$ levels at the extracellular space.

## DISCUSSION

The physiological function of APP is unknown. However growing evidence support the idea that APP may be involved in the Cu homeostasis (27). APP coordinates Cu forming bioinorganic complexes with high $K_d$ values (23), suggesting a possible in vivo relevance (17). APP contains in its structure clusters of amino acids ordinarily involved in Cu binding coordination such as histidines and cysteine. Moreover, some studies indicated that APP-deficient mice have elevated Cu levels in the liver and in cerebral cortex when compared with wild-type mice (15). In addition, CuBD of APP are capable to reduce $Cu^{2+}$ to $Cu^{1+}$ (3, 4, 14).

In this study, we evaluated whether the CuBD of APP modulates $Cu^{2+}$ neurotoxicity at the level of the hippocampus, performing intra-hippocampal injections in rats as an in vivo model. $CuCl_2$ was injected alone or co-injected with several synthetic peptides corresponding to the CuBD of human wild-type APP, human mutant APP peptides and APP ortholog of *C. elegans*. In addition, we carried out different treatments during the incubation of $CuCl_2$ with the peptides, injected immediately or preincubated overnight at 4°C or at 37°C. Due to the fact that results may be explained by the need to metallate Cu to the CuBD of APP to mediate its effect, as described by White et al. (16), the different peptides used in this work were metallated. The $Cu^{2+}$ neurotoxic effect was analyzed by the neuropathological changes observed at the injection site as well as the spatial learning acquisition using the Morris water maze task.

In all experiments, we did not find any differences between the peptides metallated or not. Moreover, we did not find any evidence that Cu-metallated CuBD of APP induces neuronal cell death in vivo, as has been recently claimed by experiments in vitro (16).

Our studies indicated that when human $APP_{135-156}$ was injected plus $CuCl_2$ it clearly protected against the $Cu^{2+}$ toxicity at both the behavioral and histological levels, showing lower escape latency scores, neuronal cell loss, and astrogliosis. To evaluate the role of Cu binding vs. the Cu-reduction ability on the CuBD of APP neuroprotective properties, we used CuBD of APP mutated in histidines or cysteine residues ($APP_{His147\rightarrow Ala/His149\rightarrow Ala}$ and $APP_{Cys144\rightarrow Ser}$). The co-injection of $CuCl_2$ plus $APP_{His147\rightarrow Ala/His149\rightarrow Ala}$ showed a similar protection to that observed with the $APP_{135-156}$ peptide. However, when $CuCl_2$ was co-injected with $APP_{Cys144\rightarrow Ser}$, the same neuroprotective effect was not observed; in fact higher escape latency values in the spatial memory test, increased hippocampal neuronal cell loss, and astrogliosis was found. Our studies indicate that the CuBD of APP protects against the $Cu^{2+}$ neurotoxicity because of its $Cu^{2+}/Cu^{1+}$ reducing capacity. Interestingly, the same dependence on the reducing activity has been observed recently (28). In that paper, it was used the CuBD of prion protein, which is able to bind and reduce copper. When $CuCl_2$ was injected in presence of the prion peptide lacking Trp residues (responsible to reduce copper), it was observed a decrease in the neuroprotective effect; however, the neuroprotection was observed with the prion peptide lacking His residues.

The specific effect observed by the injection of various divalent metals do not showed differences between the administration of the metal alone or with the metal plus $APP_{135-156}$. $CuCl_2$ shows more neurotoxicity than $ZnCl_2$; however, in both cases, no recovery was observed with the $APP_{135-156}$ injection. The fragment used in this study may binds other divalent metals (18); however, the APP reducing activity was specific for copper. Therefore, $APP_{135-156}$ only shows protective effects on rat injected with $CuCl_2$.

We also evaluate the effect of a homologue of the CuBD of human APP, the *C. elegans* ortholog $APP_{135-156\ C.\ elegans}$. This CuBD peptide present variations within the central histidine binding domain, it binds $Cu^{2+}$ and maintains the adjacent cysteine (18). The *C. elegans* peptide was co-injected with $CuCl_2$, and a neuroprotective effect was found at both the behavioral and morphological levels. These results are consistent with a previous report showing that this peptide was also neuroprotective in vitro (16).

An important point in the present work was to evaluate whether the copper-induced neurotoxicity was related to oxidative stress; specifically, it was of interest to study the presence of 3-nitrotyrosine residues, since these markers have been found in some neurodegenerative disorders. For example, in Parkinson disease (PD), it has been demonstrated that tyrosine hydroxylase, the enzyme responsible to synthetize dopamine, is a selective target for nitration after exposure to peroxinitrite, which induces the loss of the enzymatic activity (29). Likewise, α-synuclein is also a selective target for tyrosine nitration, which may be relevant to the putative role of α-synuclein in the neurodegeneration observed in PD (30). In the cerebrospinal fluid of Alzheimer's disease patients an increased concentration of 3-nitrotyrosine was found, concomitantly with decreasing cognitive functions. This suggests that activation of tyrosine nitration may play a role in the pathogenesis of Alzheimer's disease (31). In transgenic mice expressing the human familial amyotrophic lateral sclerosis-linked SOD1 mutation (a mouse model for ALS), increased nitrotyrosine levels were found, suggesting that tyrosine nitration is one in vivo aberrant property of this ALS-linked SOD1 mutant (32). In addition, hippocampal neurons showed an increased nitrotyrosine immunoreactivity after the exposure to $FeSO_4$ and $A\beta_{25-35}$ (33). Thus, it was of interest to study the presence of this oxidative stress marker, which

is induced by peroxinitrite and catalyzed by transition metals like $Cu^{2+}$ (26), and analyze if tyrosine nitration was occurring in the rat hippocampus after injection of $CuCl_2$ and if it was related to the magnitude of the hippocampal damage. We observed that the injection of $CuCl_2$ alone or $CuCl_2$ plus $APP_{Cys144\rightarrow Ser}$ induced an important immunohistochemical nitrotyrosine signal, indicating that reactive oxidative species were generated inducing oxidative stress. In contrast, the co-injection of the human wild-type APP and the APP variant peptide without histidines plus $CuCl_2$ only showed a weak signal.

The protection observed with $APP_{135-156}$ is in agreement with previous studies demonstrating neuroprotective and neurotrophic activities for soluble APP (8–13). However, such results are not in apparent agreement with previous studies that showed that the CuBD of APP in vitro (16) or in neuronal cell cultures obtained from APP knockout mice present toxic effects (34). One possible explanation for these differences may be related to the cellular $Cu^{2+}$ uptake; in fact, in the latter studies the authors did not find differences in the $Cu^{2+}$ uptake between wild-type and deficient-APP neurons; therefore, a possible increment in $Cu^{1+}$ concentration may induce toxic events, including lipid peroxidation. In contrast, in the present work we found an increased $Cu^{2+}$ uptake in the presence of the CuBD of APP peptides, which may be instrumental in decrease the extracellular $Cu^{1+}$ concentration, which in turn decreases Cu-dependent oxidative stress. For example, $APP_{Cys144\rightarrow Ser}$, which did not protect against $Cu^{2+}$ toxicity, presents a lower Cu-uptake capacity (50% less) than the wild-type $APP_{135-156}$, suggesting that the neuroprotection observed during the co-injection of the CuBD of APP plus $CuCl_2$ reflects not only a chelating property of the peptide. In fact, this is in aggrement with the idea that the intracellular milieu exhibits an overcapacity for Cu-chelation (35) and thus an increase incorporation of Cu may limit the toxicity of the metal in the extracellular milieu. Consistent with this idea, we observed an increment in the $Cu^{2+}$ uptake in the presence of APP peptides that present protection of both spatial memory capacities and hippocampal damage.

$Cu^{2+}/Cu^{+}$ is an essential micronutrient for humans, as it constitutes an important component of various redox enzymes. However, free $Cu^{2+}/Cu^{+}$ is a toxic ion, and both excess and deficiency lead to disorders such as Wilson's and Menkes's diseases (36). In eukaryotic cells, the incorporation of $Cu^{2+}$ occurs in a reduced state, via the $Cu^{1+}$-transporter hCtr1 (37, 38). Therefore, the Cu-reducing activity of APP might serve in a favorable physiological function as a cell membrane $Cu^{2+}$-reductase similar to Fre1 in yeast (39), modulating the amount of $Cu^{1+}$ for subsequent uptake by Cu-transport proteins. In unfavorable conditions, an increase of APP on the cell surface may increase the reduction of $Cu^{2+}$ to $Cu^{1+}$, generating an enhancement of $Cu^{1+}$ levels and free radicals and consequently causing an increased oxidative damage (4, 14, 40).

In conclusion, our data indicate that the CuBD of APP can modulate $Cu^{2+}/Cu^{+}$ availability in vivo, supporting the notion that the APP is involved in $Cu^{2+}/Cu^{+}$ homeostasis (4, 17, 41, 42).

## ACKNOWLEDGMENTS

We thank Dr. Rocío Foncea from the Department of Nutrition, Faculty of Medicine, Catholic University of Chile, for her kind gift of the anti-nitrotyrosine antibody. This work was supported by the International Copper Association (ICA, New York, NY), FONDAP-Biomedicine grant Nº 13980001, and the Millennium Institute of Fundamental and Applied Biology (MIFAB).

## REFERENCES


1. Hardy, J., and Selkoe, D. J. (2002) The amyloid hypothesis of Alzheimer's disease: progress and problems on the road to therapeutics. *Science* **297,** 353–356

2. Atwood, C. S., Scarpa, R. C., Huang, X., Moir, R. D., Jones, W. D., Fairlie, D. P., Tanzi, R. E., and Bush, A. I. (2000) Characterization of copper interactions with alzheimer amyloid beta peptides: identification of an attomolar-affinity copper binding site on amyloid beta1-42. *J. Neurochem.* **75,** 1219–1233

3. Multhaup, G., Schlicksupp, A., Hesse, L., Beher, D., Ruppert, T., Masters, C. L., and Beyreuther, K. (1996) The amyloid precursor protein of Alzheimer's disease in the reduction of copper (II) to copper (I). *Science* **271,** 1406–1409

4. Ruiz, F. H., Gonzalez, M., Bodini, M., Opazo, C., and Inestrosa, N. C. (1999) Cysteine 144 is a key residue in the copper reduction by the β-amyloid precursor protein. *J. Neurochem.* **73,** 1288–1292

5. Wasco, W., Bupp, K., Magendantz, M., Gusella, J. F., Tanzi, R. E., and Solomon, F. (1992) Identification of a mouse brain cDNA that encodes a protein related to the Alzheimer disease-associated amyloid β protein precursor. *Proc. Natl. Acad. Sci. USA* **89,** 10758–10762

6. Slunt, H. H., Thinakaran, G., von Koch, C., Lo, A. C. Y., Tanzi, R. E., and Sisodia, S. S. (1994) Expression of ubiquitous, cross-reactive homologue of the mouse β-amyloid precursor protein (APP). *J. Biol. Chem.* **269,** 2637–2644

7. Daigle, I., and Li, C. (1993) APL-1, a *Caenorhabditis elegans* gene encoding a protein related to the human β-amyloid protein precursor. *Proc. Natl. Acad. Sci. USA* **90,** 12045–12049

8. Milward, E., Papadopoulos, R., Fuller, S. J., Moir, R. D., Small, D., Beyreuther, K., and Masters, C. L. (1992) The amyloid protein precursor of Alzheimer's disease is a mediator of the effects of nerve growth factor on neurite outgrowth. *Neuron* **9,** 129–137

9. Alvarez, J., Moreno, R. D., Llanos, O., Inestrosa, N. C., Brandan, E., Colby, T., and Esch, F. S. (1992) Axonal sprouting induced in the sciatic nerve by the amyloid precursor protein (APP) and other antiproteases. *Neurosci. Lett.* **144,** 130–134

10. Mattson, M. P., Cheng, B., Culwell, A. R., Esch, F. S., Lieberburg, I., and Rydel, R. E. (1993) Evidence for excitoprotective and intraneuronal calcium-regulating roles for secreted forms of the β-amyloid precursor protein. *Neuron* **10,** 243–254

11. Small, D. H., Nurcombe, V., Reed, G., Clarris, H., Moir, R., Beyreuther, K., and Masters, C. L. (1994) A heparin-binding domain in the amyloid protein precursor of Alzheimer's disease is involved in the regulation of neurite outgrowth. *J. Neurosci.* **14,** 2117–2127

12. Alvarez, J., Moreno, R. D., and Inestrosa, N. C. (1995) Mitosis of Schwann cells and demyelination are induced by the amyloid precursor protein and other protease inhibitors in the rat sciatic nerve. *Eur. J. Neurosci.* **7,** 152–159

13. Moreno, R. D., Inestrosa, N. C., Culwell, A. R., and Alvarez, J. (1996) Sprouting and abnormal contact of nonmedullated axons, and deposition of extracellular material induced by the amyloid precursor protein (APP) and other protease inhibitors. *Brain Res.* **718,** 13–24

14. Opazo, C., Barría, M. I., Ruiz, F., and Inestrosa, N. C. (2003) Copper reduction by copper binding proteins and its relation to neurodegenerative diseases. *Biometals* **16,** 91–98

15. White, A. R., Reyes, R., Mercer, J. F., Camakaris, J., Zheng, H., Bush, A. I., Multhaup, G., Beyreuther, K., Masters, C. L., and Cappai, R. (1999a) Copper levels are increased in the cerebral cortex and liver of APP and APLP2 knockout mice. *Brain Res.* **842,** 439–444

16. White, A. R., Multhaup, G., Galatis, D., McKinstry, W. J., Parker, M. W., Pipkorn, R., Beyreuther, K., Masters, C. L., and Cappai, R. (2002) Contrasting, species-dependent modulation of copper-mediated neurotoxicity by the Alzheimer's disease amyloid precursor protein. *J. Neurosci.* **22,** 365–376

17. Maynard, C. J., Cappai, R., Volitakis, I., Cherny, R. A., White, A. R., Beyreuther, K., Masters, C. L., Bush, A. I., and Li, Q. X. (2002) Overexpression of Alzheimer's disease amyloid-β opposes the age-dependent elevations of brain copper and iron. *J. Biol. Chem.* **277,** 44670–44676

18. Simons, A., Ruppert, T., Schmidt, C., Schlicksupp, A., Pipkorn, R., Reed, J., Masters, C. L., White, A. R., Cappai, R., Beyreuther, K., et al. (2002) Evidence for a copper-binding superfamily of the amyloid precursor protein. *Biochemistry* **41,** 9310–9320

19. Paxinos, G., and Watson, C. (1986). *The Rat Brain in Stereotaxic Coordinates* (2nd ed.),Academic Press, New York

20. Morris, R. G. M. (1984) Developments of a water maze procedure for studing spatial learning in the rat. *J.Neurosci Meth.* **11,** 47–60

21. Côté, S. L., Ribeiro-Da-Silva, A., and Cuello, A. C. (1993) *Immunocytochemistry II*, (Cuello, A. C. ed), John Wiley & Sons, New York

22. Bradford, M. M. (1976) A rapid and sensitive for the quantitation of microgram quantitites of protein utilizing the principle of protein-dye binding. *Anal. Biochem.* **72,** 248–254

23. Hesse, L., Beher, D., Masters, C. L., and Multhaup, G. (1994) The β A4 amyloid precursor protein binding to copper. *FEBS Lett.* **349,** 109–116

24. Mandel, R. J., Gage, F. H., and Thal, L. J. (1989) Spatial learning in rats: correlation with cortical choline acetyltransferase and improvement with NGF following NBM damage. *Exp. Neurol.* **104,** 208–217

25. Chacón, M. A., Reyes, A. E., and Inestrosa, N. C. (2003a) Acetylcholinesterase induces neuronal cell loss, astrocyte hypertrophy and behavioral deficits in mammalian hippocampus. *J. Neurochem.* **87,** 195–204

26. Beckman, J. S. (1996) Oxidative damage and tyrosine nitration from peroxynitrite. *Chem. Res. Toxicol.* **9,** 836–844

27. Bush, A. I. (2003) The metallobiology of Alzheimer's disease. *Trends Neurosci.* **26,** 207–214

28. Chacón, M. A., Barría, M. I., Lorca, R., Huidobro-Toro, J. P., and Inestrosa, N. C. (2003b) A human prion protein peptide ($PrP_{(59-91)}$) protects against copper neurotoxicity. *Mol. Psychiatry* **8,** 853–862

29. Ara, J., Przedborski, S., Naini, A. B., Jackson-Lewis, V., Trifiletti, R. R., Horwitz, J., and Ischiropoulos, H. (1998) Inactivation of tyrosine hydroxylase by nitration following exposure to peroxynitrite and 1-methyl-4-phenyl-1,2,3,6-tetrahydropyridine (MPTP). *Proc. Natl. Acad. Sci. USA* **95,** 7659–7663

30. Przedborski, S., Chen, Q., Vila, M., Giasson, B. I., Djaldatti, R., Vukosavic, S., Souza, J. M., Jackson-Lewis, V., Lee, V. M., and Ischiropoulos, H. (2001) Oxidative post-translational modifications of alpha-synuclein in the 1-methyl-4-phenyl-1,2,3,6-tetrahydropyridine (MPTP) mouse model of Parkinson's disease. *J. Neurochem.* **76,** 637–640

31. Tohgi, H., Abe, T., Yamazaki, K., Murata, T., Ishizaki, E., and Isobe, C. (1999) Alterations of 3-nitrotyrosine concentration in the cerebrospinal fluid during aging and in patients with Alzheimer's disease. *Neurosci. Lett.* **269,** 52–54

32. Bruijn, L. I., Beal, M. F., Becher, M. W., Schulz, J. B., Wong, P. C., Price, D. L., and Cleveland, D. W. (1997) Elevated free nitrotyrosine levels, but not protein-bound nitrotyrosine or hydroxyl radicals, throughout amyotrophic lateral sclerosis (ALS)-like disease implicate tyrosine nitration as an aberrant in vivo property of one familial ALS-linked superoxide dismutase 1 mutant. *Proc. Natl. Acad. Sci. USA* **94,** 7606–7611

33. Mattson, M. P., Goodman, Y., Luo, H., Fu, W., and Furukawa, K. (1997) Activation of NF-kappaB protects hippocampal neurons against oxidative stress-induced apoptosis: evidence for induction of manganese superoxide dismutase and suppression of peroxynitrite production and protein tyrosine nitration. *J. Neurosci. Res.* **49,** 681–697

34. White, A. R., Multhaup, G., Maher, F., Bellingham, S., Camakaris, J., Zheng, H., Bush, A. I., Beyreuther, K., Masters, C. L., and Cappai, R. (1999b) The Alzheimer's disease amyloid precursor protein modulates copper-induced toxicity and oxidative stress in primary neuronal cultures. *J. Neurosci.* **19,** 9170–9179

35. Rae, T. D., Schmidt, P. J., Pufahl, R. A., Culotta, V. C., and O'Halloran, T. V. (1999). Undetectable intracellular free copper: the requeriment of a copper chaperone for superoxide dismutase. *Science* **284,** 805-809

36. Harris, E. D. (2000) Cellular copper transport and metabolism. *Annu. Rev. Nutr.* **20,** 291–310

37. Zhou, B., and Gitschier, J. (1997) hCTR1: a human gene for copper uptake identified by complementation in yeast. *Proc. Natl. Acad. Sci. USA* **94,** 7481–7486

38. Lee, J., Peña, M. M., Nose, Y., and Thiele, D. J. (2002) Biochemical characterization of the human copper transporter Ctr1. *J. Biol. Chem.* **277,** 4380–4387

39. Georgatson, E., Mavrogiannis, L. A., Fragiadakis, G. S., and Alexandraki, D. (1997) The yeast Fre1P/Fre2P cupric reductases facilitate copper uptake and are regulated by the copper-modulated Mac1P activator. *J. Biol. Chem.* **272,** 13786–13792

40. Davies, K. J. A., Delsignore, M. A., and Lin, S. W. (1987) Protein damage and degradation by oxygen radicals. II. Modification of amino acids. *J. Biol. Chem.* **262,** 9902–9907

41. Opazo, C., Huang, X., Cherny, R. A., Moir, R. D., Roher, A. E., White, A. R., Cappai, R., Masters, C. L., Tanzi, R. E., Inestrosa, N. C., et al. (2002) Metalloenzyme-like activity of Alzheimer's disease β-amyloid. Cu-dependent catalytic conversion of dopamine, cholesterol, and biological reducing agents to neurotoxic $H_2O_2$. *J. Biol. Chem.* **277,** 40302–40308

42. Barnham, K. J., McKinstry, W. J., Multhaup, G., Galatis, D., Morton, C. J., Curtain, C. C., Williamson, N. A., White, A. R., Hinds, M. G., Norton, R. S., Beyreuther, K., Masters, C. L., Parker, M. W., and Cappai, R. (2003) Structure of the Alzheimer's disease amyloid precursor protein copper binding domain. A regulator of neuronal copper homeostasis. *J. Biol. Chem.* **278,** 17401-17407

*Received January 13, 2004; accepted July 2, 2004.*

**Fig. 1**

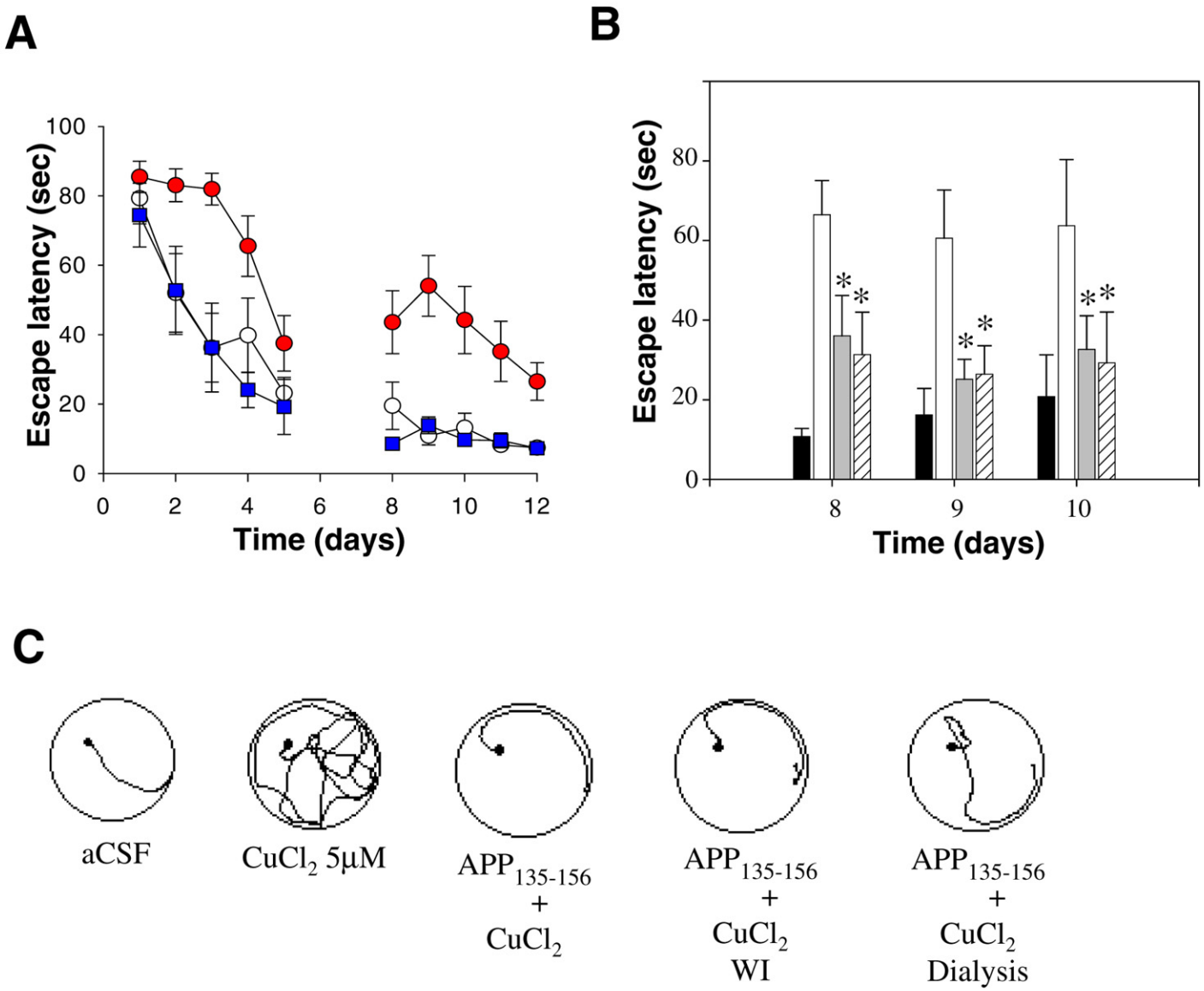


**Figure 1. Human $APP_{135-156}$ protects spatial memory acquisition against $Cu^{2+}$ neurotoxicity.** ***A*****)** Escape latency scores along 2 wk of training of rats injected with aCSF (white circles, *n*=5), 5 μM $CuCl_2$ (red circles, *n*=5) and 5 μM $CuCl_2$ plus 5 μM of human $APP_{135-156}$ (blue squares, *n*=6). ***B*****)** Escape latency values of representative days of training of rats injected with aCSF (black bars), 5 μM $CuCl_2$ (white bars), 5 μM $CuCl_2$ plus 5 μM of human $APP_{135-156}$ in different conditions, without incubation (gray bars, *n*= 5) and with preincubation and dialysis (dashed bars, *n*=5; see Materials and Methods). ***C*****)** Representative swimming paths at day 8 of training. $*P < 0.05$.

**Fig. 2**

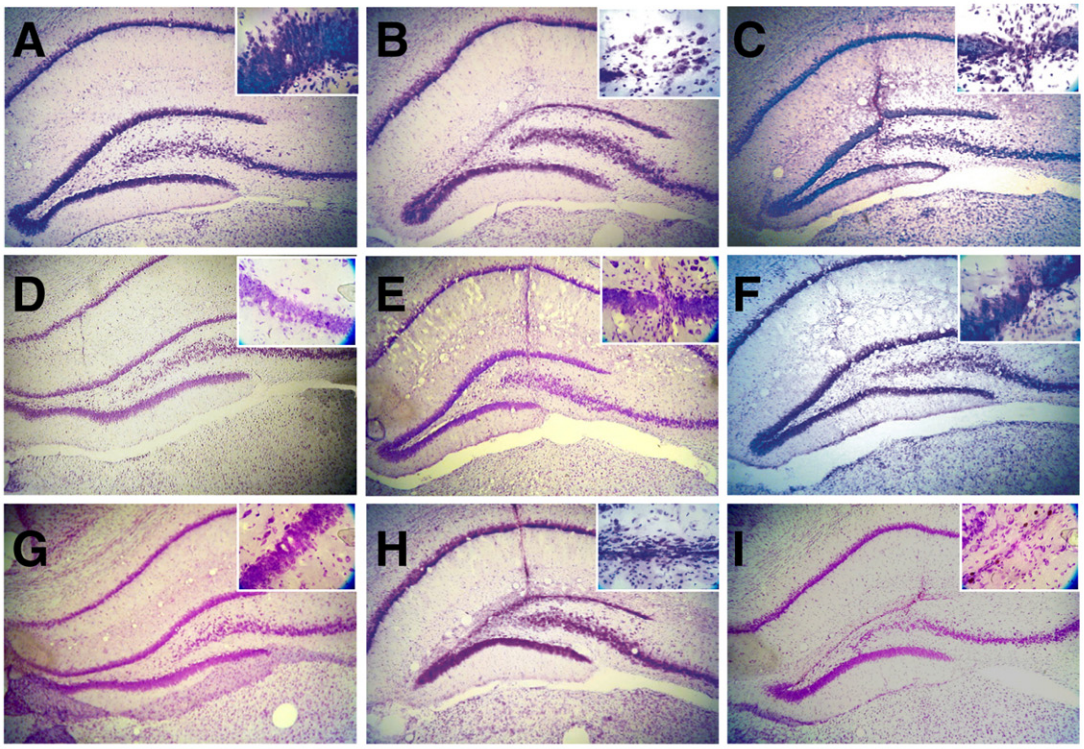
A
B
C
D
E
F
G
H
I

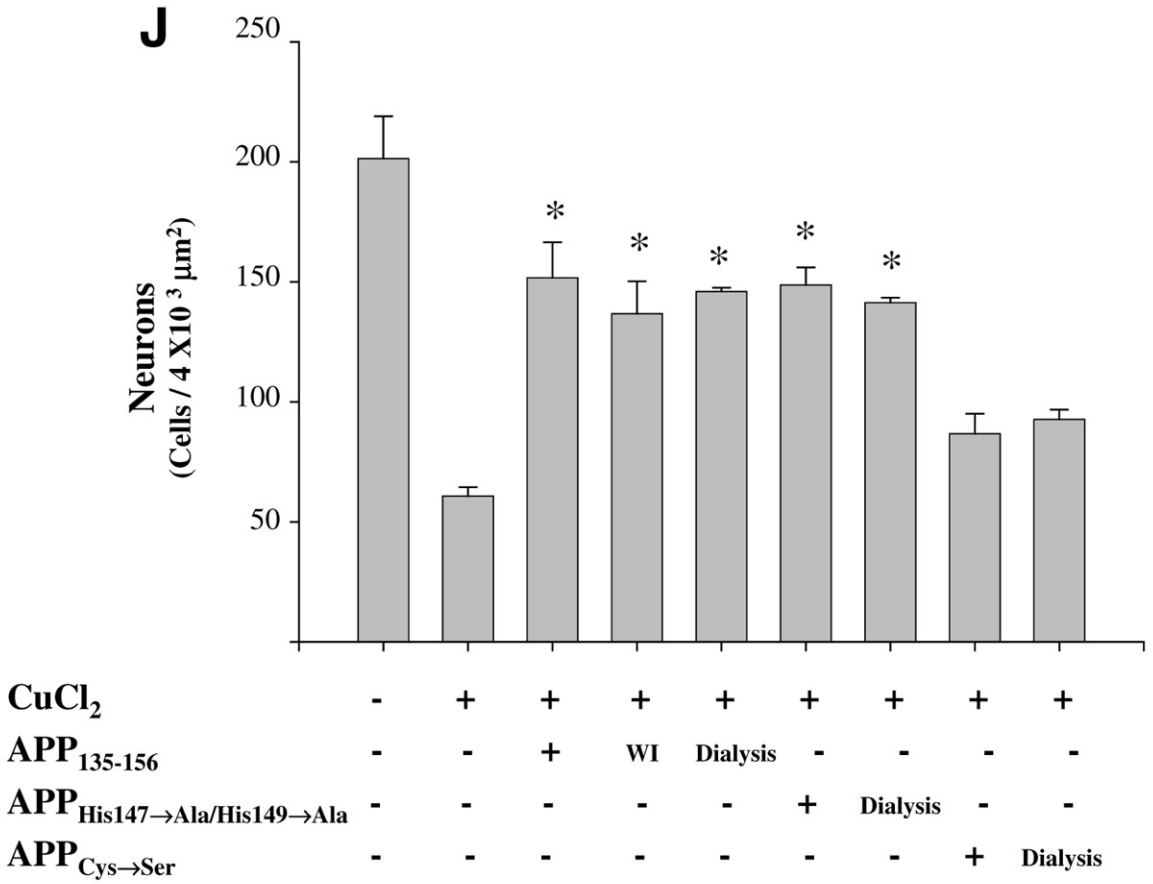
J
Neurons
(Cells / 4 X10 3 µm2)
250
200
150
100
50
*
CuCl2 - + + + + + + + +
APP135-156 - - + WI Dialysis - - - -
APPHis147→Ala/His149→Ala - - - - - + Dialysis - -
APPCys→Ser - - - - - - - + Dialysis

**Figure 2. Effect of different CuBD of APP on hippocampal morphological changes generated by $Cu^{2+}$.** Histological analysis by Nissl staining of coronal brain sections of rats injected with the following: ***A***) aCSF; ***B***) 5 μM $CuCl_2$; ***C***) 5 μM $CuCl_2$ plus 5 μM of human $APP_{135-156}$ (preincubated O.N. at 4°C); ***D***) 5 μM $CuCl_2$ plus 5 μM of human $APP_{135-156}$ (without incubation, WI); ***E***) 5 μM $CuCl_2$ plus 5 μM of human $APP_{135-156}$ (dialyzed); ***F***) 5 μM $CuCl_2$ plus 5 μM $APP_{His147\rightarrow Ala/His149\rightarrow Ala}$ (preincubated O.N. at 4°C); ***G***) 5 μM $CuCl_2$ plus 5 μM $APP_{His147\rightarrow Ala/His149\rightarrow Ala}$ (preincubated at 37°C and dialyzed); ***H***) 5 μM $CuCl_2$ plus 5 μM $APP_{Cys144\rightarrow Ser}$ (preincubated O.N. at 4°C); ***I***) 5 μM $CuCl_2$ plus 5 μM $APP_{Cys144\rightarrow Ser}$ (preincubated O.N. at 37°C and dialyzed). Panels are x4 magnification. Insets are x40 magnification. ***J***) Graph corresponds to neuronal density at injection site of each treatment quantified with the Image Pro-Express software. $*P < 0.05$.

**Fig. 3**

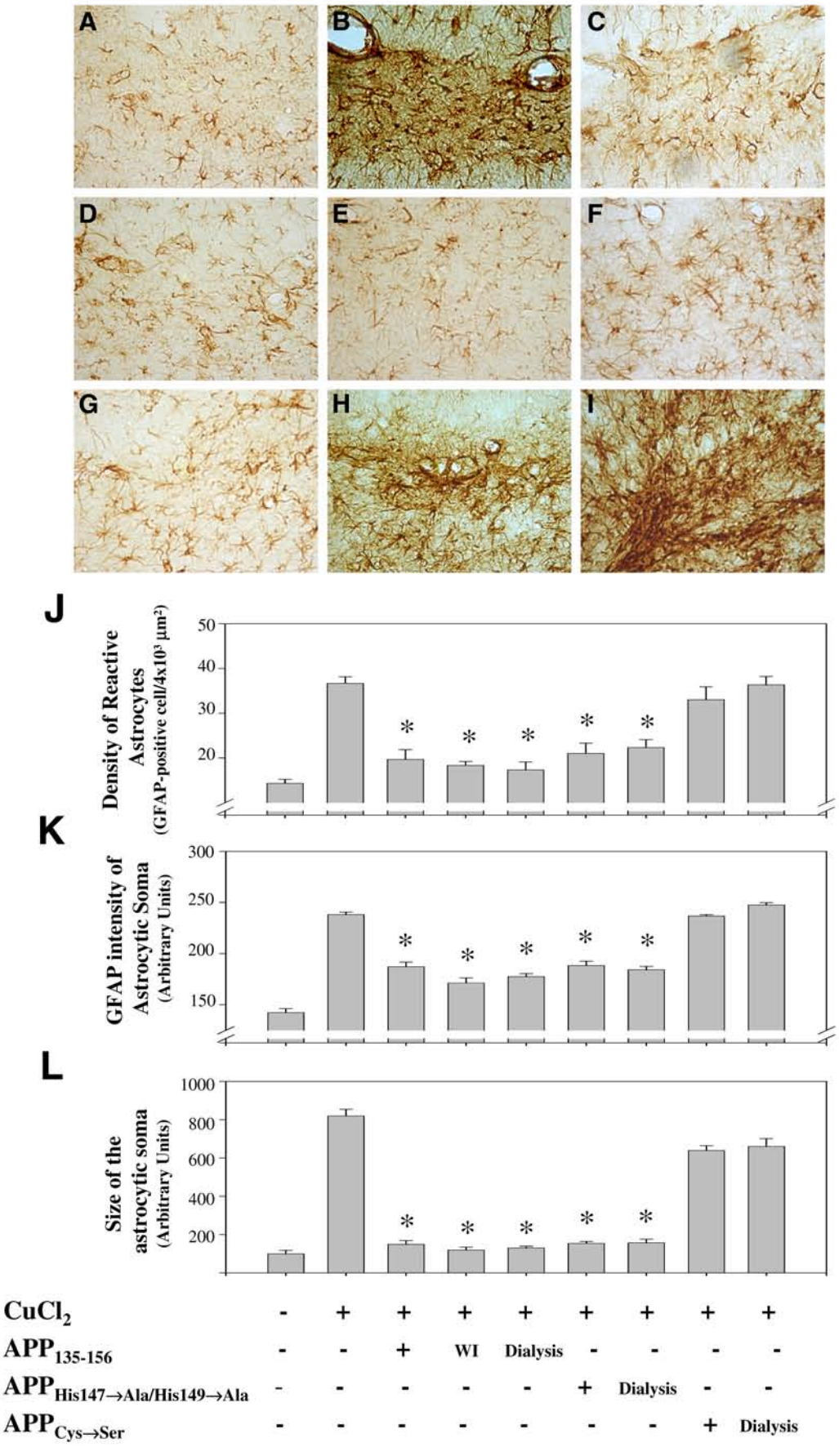
A
B
C
D
E
F
G
H
I
J
Density of Reactive Astrocytes
(GFAP-positive cell/4x10³ μm²)
50
40
30
20
K
GFAP intensity of Astrocytic Soma
(Arbitrary Units)
300
250
200
150
L
Size of the astrocytic soma
(Arbitrary Units)
1000
800
600
400
200
CuCl2 - + + + + + + + +
APP135-156 - - + WI Dialysis - - - -
APPHis147→Ala/His149→Ala - - - - - + Dialysis - -
APPCys→Ser - - - - - - - + Dialysis

**Figure 3. Effect of different CuBD of APP on astrocytic density and number of hypertrophic astrocytes induced by $Cu^{2+}$ neurotoxicity.** Analysis of reactive astrocytes by GFAP immunohistochemistry in the upper leaf of the dentate gyrus of animals injected with the following: ***A***) aCSF; ***B***) 5 μM $CuCl_2$; ***C***) 5 μM $CuCl_2$ plus 5 μM of human $APP_{135\text{-}156}$ (preincubated O.N. at 4°C); ***D***) 5 μM $CuCl_2$ plus 5 μM of human $APP_{135\text{-}156}$ (without incubation, WI); ***E***) 5 μM $CuCl_2$ plus 5 μM of human $APP_{135\text{-}156}$ (preincubated O.N. at 37°C and dialyzed); ***F***) 5 μM $CuCl_2$ plus $APP_{His147\rightarrow Ala/His149\rightarrow Ala}$ (preincubated O.N. at 4°C); ***G***) 5 μM $CuCl_2$ plus $APP_{His147\rightarrow Ala/His149\rightarrow Ala}$ (preincubated O.N. at 37°C and dialyzed); ***H***) 5 μM $CuCl_2$ plus 5 μM $APP_{Cys144\rightarrow Ser}$ (preincubated O.N. at 4°C); ***I***) 5 μM $CuCl_2$ plus 5 μM $APP_{Cys144\rightarrow Ser}$ (preincubated O.N. at 37°C and dialyzed). Micrographs correspond at x40 magnification. Graphs represent digital quantification by SigmaScan Pro of: ***J***) density of reactive astrocytes; ***K***) GFAP intensity of astrocytic soma; ***L***) size of the astrocytic soma. $*P < 0.05$.

**Fig. 4**

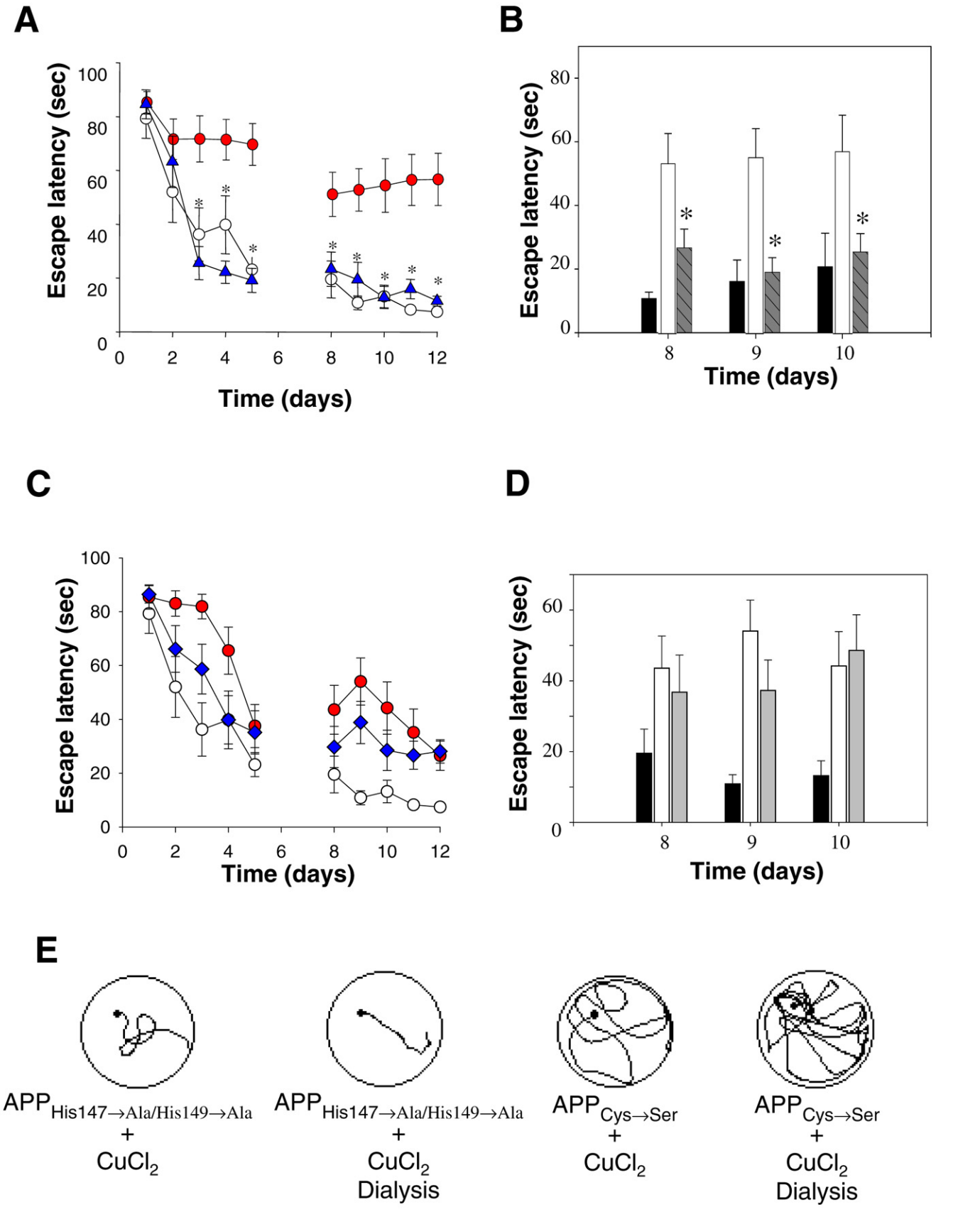
A
Escape latency (sec)
Time (days)
B
Escape latency (sec)
Time (days)
C
Escape latency (sec)
Time (days)
D
Escape latency (sec)
Time (days)
E
APP His147→Ala/His149→Ala + CuCl2
APP His147→Ala/His149→Ala + CuCl2 Dialysis
APP Cys→Ser + CuCl2
APP Cys→Ser + CuCl2 Dialysis

**Figure 4. Effect of mutant $APP_{135-156}$ on spatial memory against $Cu^{2+}$ neurotoxicity.** ***A*****)** Escape latency values of trained rats injected with aCSF (white circles, *n*=5), 5 μM $CuCl_2$ (red circles, *n*=5), and 5 μM $CuCl_2$ plus 5 μM $APP_{His147\rightarrow Ala/His149\rightarrow Ala}$ (blue triangles, *n*=5) (all mixtures were preincubated O.N. at 4°C). ***B*****)** Escape latency values of representative days of training of rats injected with aCSF (black bars), 5 μM $CuCl_2$ (white bars), 5 μM $CuCl_2$ plus 5 μM $APP_{His147\rightarrow Ala/His149\rightarrow Ala}$ (dashed bars, *n*=5) (preincubated O.N. at 37°C and dialyzed). ***C*****)** Escape latency values of rats injected with with aCSF (white circles, *n*=5), 5 μM $CuCl_2$ (red circles, *n*= 5), 5 μM 5 μM $CuCl_2$ plus 5 μM 5 μM $APP_{Cys144\rightarrow Ser}$ (blue rhombus, *n*=5). ***D*****)** Escape latency values of representative days of training of rats injected with aCSF (black bars), 5 μM $CuCl_2$ (white bars), and 5 μM $CuCl_2$ plus 5 μM $APP_{Cys144\rightarrow Ser}$ (gray bars, *n*=5) (preincubated O.N. at 37°C and dialyzed). ***E*****)** Representative swimming paths at day 8 of training. $*P < 0.05$.

**Fig. 5**

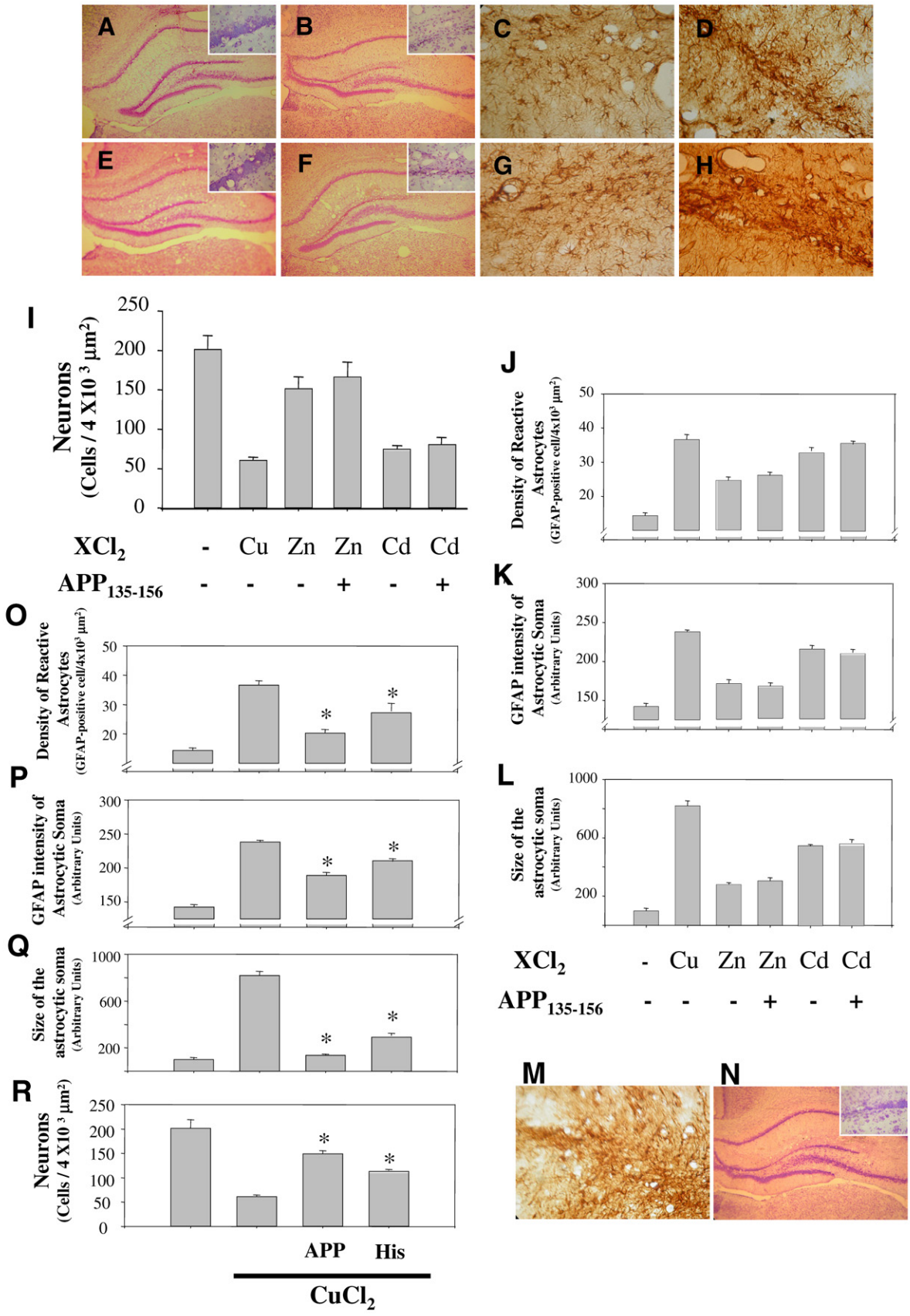
A
B
C
D
E
F
G
H
I
Neurons (Cells / 4 X10 3 µm2)
250
200
150
100
50
0
XCl2 - Cu Zn Zn Cd Cd
APP135-156 - - - + - +
J
Density of Reactive Astrocytes (GFAP-positive cell/4x10³ µm²)
50
40
30
20
K
GFAP intensity of Astrocytic Soma (Arbitrary Units)
300
250
200
150
L
Size of the astrocytic soma (Arbitrary Units)
1000
600
200
XCl2 - Cu Zn Zn Cd Cd
APP135-156 - - - + - +
M
N
O
Density of Reactive Astrocytes (GFAP-positive cell/4x10³ µm²)
50
40
30
20
*
*
P
GFAP intensity of Astrocytic Soma (Arbitrary Units)
300
250
200
150
*
*
Q
Size of the astrocytic soma (Arbitrary Units)
1000
600
200
*
*
R
Neurons (Cells / 4 X10 3 µm2)
250
200
150
100
50
0
*
*
APP
His
CuCl2

**Figure 5. Specific neuroprtective effect to $APP_{135-156}$ on hippocampal morphology against $Cu^{2+}$ toxicity.** Coronal sections of rat injected with; 5μM $ZnCl_2$ alone (***A*** and ***C***), ***B*** and ***D*** 125nM $CdCl_2$ alone. ***E*** and ***G*****)** $ZnCl_2$ plus 5 μM $APP_{135-156}$ . ***F*** and ***H*****)** $CdCl_2$ plus 5 μM $APP_{135-156}$. ***A***, ***B***, ***E***, ***F***, and ***N*****)** Nissl staining Panels are x4 magnification. Insets are x40 magnification. ***C***, ***D***, ***G***, ***H***, and ***M*****)** GFAP immunohistochemistry Panels are x4 magnification. ***I*****)** Graph corresponds to quantification of the neuronal density of the micrographs shown in ***A***, ***B***, ***E***, and ***F***. Graphs are digital quantification by SigmaScan Pro of ***J***, density of reactive astrocytes; ***K*****)** GFAP intensity of astrocytic soma; ***L*****)** size of astrocytic soma. ***M*** and ***N*****)** Slices of rats injected with Histidine 15 μM plus $CuCl_2$ 5 μM. ***O***, ***P***, and ***Q*****)** Analysis of reactive astrocytes by GFAP immunohistochemistry (same parameters of ***J***, ***K,*** and ***L***). ***R*****)** Digital quantification of neuronal loss cells in upper leaf of dentate gyrus. $^*P < 0.05$.

**Fig. 6**

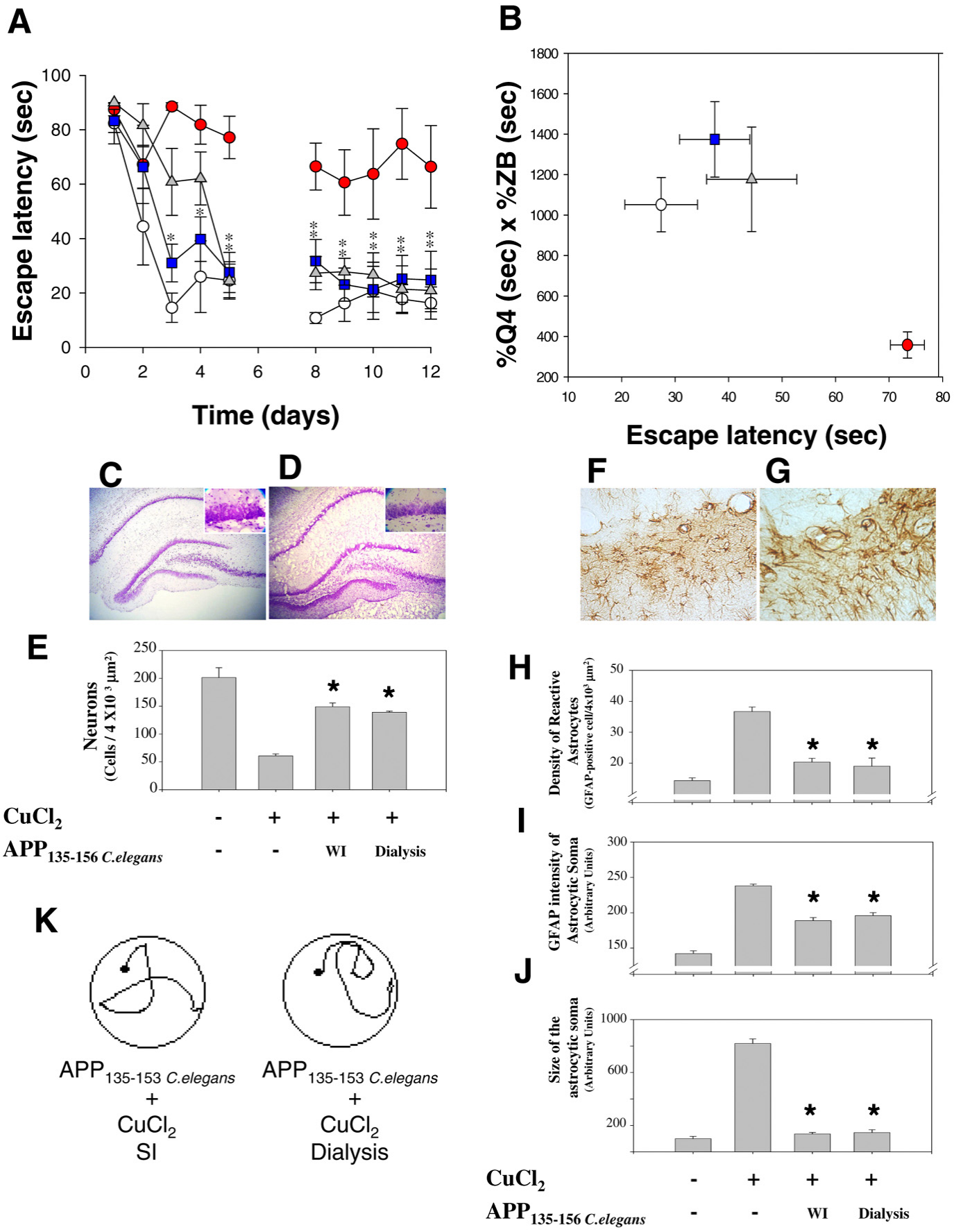
A
Escape latency (sec)
Time (days)
B
%Q4 (sec) x %ZB (sec)
Escape latency (sec)
C
D
F
G
E
Neurons
(Cells / 4 X10 ³ µm²)
CuCl2
APP135-156 C.elegans
WI
Dialysis
H
Density of Reactive Astrocytes
(GFAP-positive cell/4x10³ µm²)
I
GFAP intensity of Astrocytic Soma
(Arbitrary Units)
J
Size of the astrocytic soma
(Arbitrary Units)
K
APP135-153 C.elegans + CuCl2 SI
APP135-153 C.elegans + CuCl2 Dialysis

**Figure 6. $APP_{135-156}$ of C.elegans protects spatial memory acquisition and hippocampal morphology against $Cu^{2+}$ neurotoxicity.** ***A)*** Escape latency values of rats injected with aCSF (white circles, *n*=5), 5 μM $CuCl_2$ (red circles, *n*=5), 5 μM $CuCl_2$, and 5 μM $APP_{135-156}$ of *C.elegans* without incubation treatment (gray triangles, *n*=5) and with O.N. incubation at 37°C and dialysis (blue squares, *n*=5). ***B)*** Spatial acuity displayed by rats injected as described in ***A***. ***C*** and ***D*)** Nissl staining of coronal brain sections of rats injected with 5 μM $CuCl_2$ plus 5 μM $APP_{135-156}$ of *C.elegans* without incubation (WI) (***C***); or preincubated O.N. at 37°C and dialyzed (***D***). Panels are x4 magnification. Insets are x40 magnification. ***E*)** Graph corresponds to quantification of the neuronal density of micrographs shown in ***C*** and ***D***. ***F*** and ***G*)** Analysis of reactive astrocytes by GFAP immunohistochemistry in the upper leaf of the dentate gyrus of animals injected with 5 μM $CuCl_2$ plus 5 μM $APP_{135-156}$ of *C. elegans* without incubation (***F***) or dialyzed (***G*)**. Graphs represent digital quantification by SigmaScan Pro of: ***H*)** density of reactive astrocytes; ***I*)** GFAP intensity of astrocytic soma; ***J*)** size of the astrocytic soma. ***K*)** Representative swimming paths at day 8 of training. $^*P < 0.05$.

**Fig. 7**

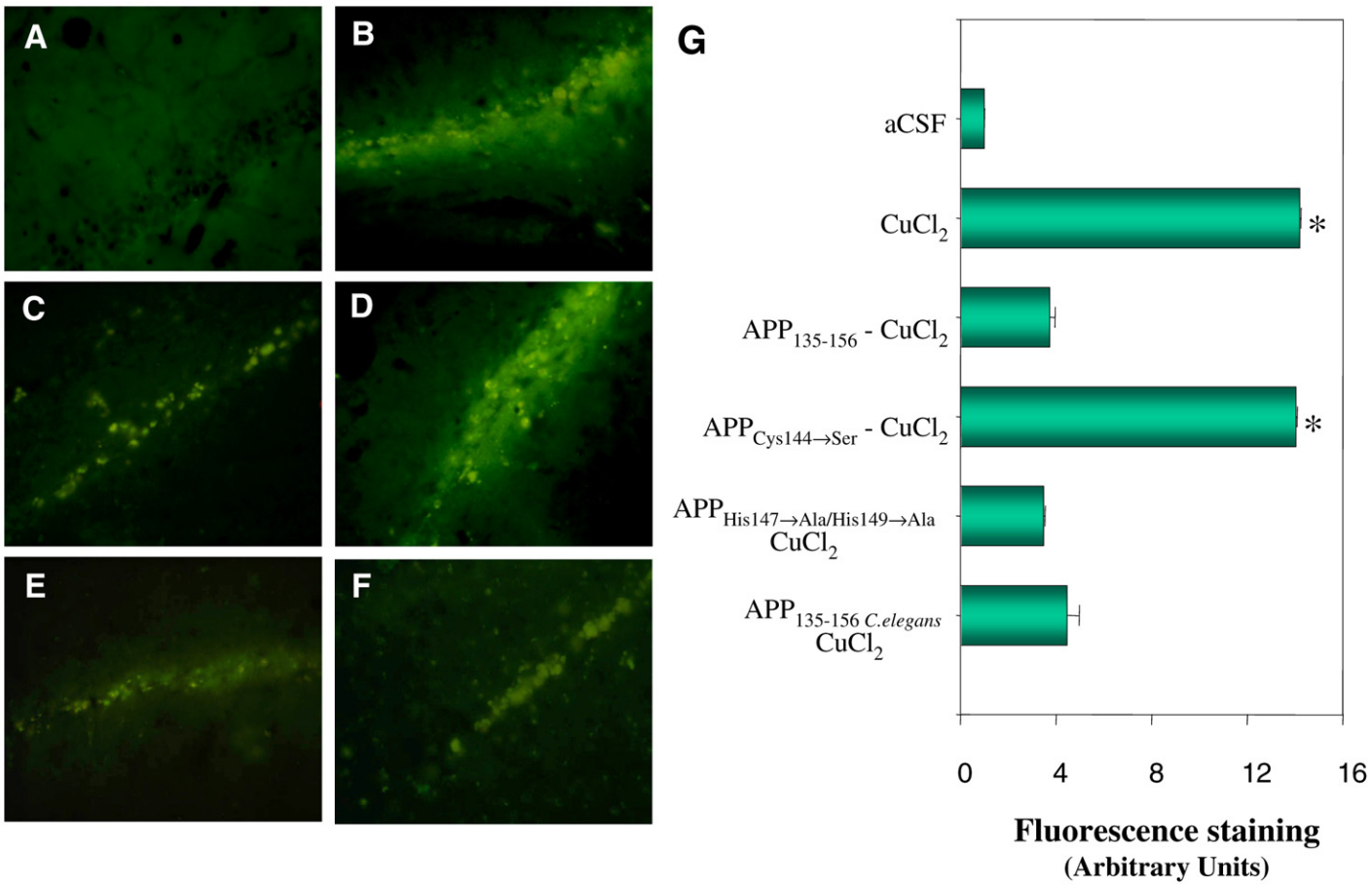


**Figure 7. Effect of different CuBD of APP and $Cu^{2+}$ in the nitrotyrosine signal in rat hippocampi.** Nitrotyrosine immunoflorescence of coronal brain sections of rats injected with the following: ***A***) aCSF; ***B***) 5 μM $CuCl_2$; ***C***) 5 μM $CuCl_2$ plus 5 μM of human $APP_{135-156}$ ; ***D***) 5 μM $CuCl_2$ plus 5 μM $APP_{Cys144\rightarrow Ser}$; ***E***) 5 μM $CuCl_2$ plus 5 μM $APP_{His147\rightarrow Ala/His149\rightarrow Ala}$; ***F***) 5 μM $CuCl_2$ plus 5 μM $APP_{135-156\ C.elegans}$. ***G***) Graph represents a digital quantification of anti-nitrotyrosine staining performed with the Image Tool software. $^*P < 0.05$.

**Fig. 8**

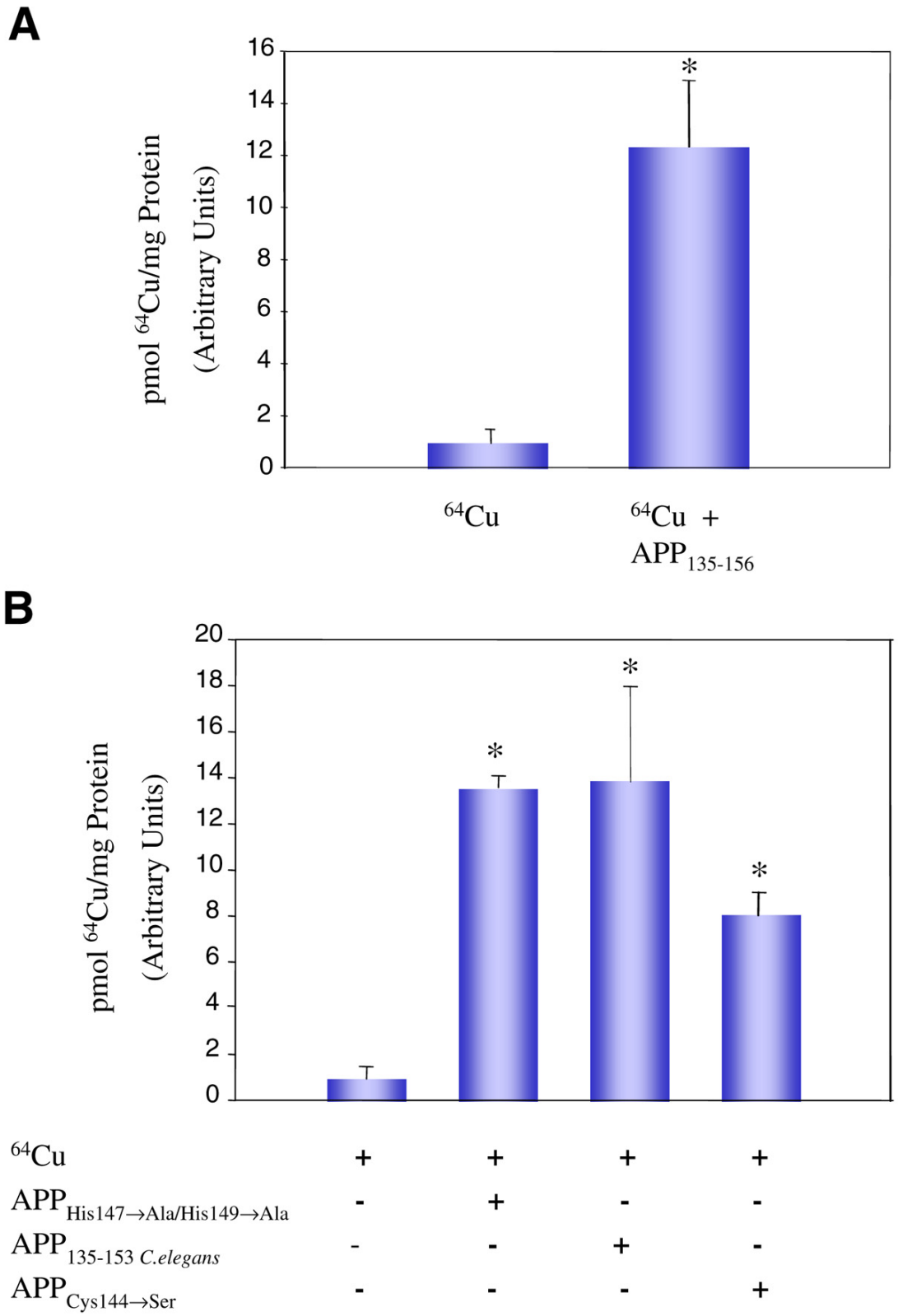


**Figure 8. CuBD APP increases the $Cu^{2+}$ uptake in vivo.** ***A*** and ***B*)** Rats were injected in dorsal hippocampus with 50 µM [$^{64}\gamma$]-Cu (4.1 mCi/mg) without or with 50 µM of different CuBD APP (human $APP_{135-156}$, $APP_{His147\rightarrow Ala/His149\rightarrow Ala}$, $APP_{Cys144\rightarrow Ser}$ and $APP_{135-156\ C.elegans}$). After 14 h, radioactivity associated to hippocampus region was determined in a γ-counter as described in Materials and Methods. *$P < 0.05$.